



CHORUS

This is the accepted manuscript made available via CHORUS. The article has been published as:

Polaron-to-Polaron Transitions in the Radio-Frequency Spectrum of a Quasi-Two-Dimensional Fermi Gas

Y. Zhang, W. Ong, I. Arakelyan, and J. E. Thomas

Phys. Rev. Lett. **108**, 235302 — Published 8 June 2012

DOI: [10.1103/PhysRevLett.108.235302](https://doi.org/10.1103/PhysRevLett.108.235302)

Polaron-to-polaron transitions in the radio-frequency spectrum of a quasi-two-dimensional Fermi gas

Y. Zhang^{1,2}, W. Ong^{1,2}, I. Arakelyan^{1,2}, and J. E. Thomas¹

¹*Department of Physics, North Carolina State University, Raleigh, NC 27695, USA and*

²*Department of Physics, Duke University, Durham, NC 27708, USA*

(Dated: April 19, 2012)

We measure radio-frequency spectra for a two-component mixture of a ⁶Li atomic Fermi gas in a quasi-two-dimensional regime with the Fermi energy comparable to the energy level spacing in the tightly confining potential. Near the Feshbach resonance, we find that the observed resonances do not correspond to transitions between confinement-induced dimers. The spectral shifts can be fit by assuming transitions between noninteracting polaron states in two dimensions.

PACS numbers: 03.75.Ss

Quantum degenerate atomic Fermi gases, with magnetically controlled interactions, are ideally suited for exploring pairing interactions in reduced dimensions [1–6]. Near a broad collisional (Feshbach) resonance, a two-component gas in three dimensions can be continuously tuned from a Bardeen-Cooper-Schrieffer (BCS) superfluid, which exhibits weakly bound Cooper pairs, to a resonant strongly interacting superfluid and finally to a Bose-Einstein condensate (BEC) of molecular dimers. Since 2002, degenerate strongly interacting Fermi gases have been studied in three-dimensional (3D) geometries, providing a paradigm for strongly interacting systems in nature, from high temperature superconductors to nuclear matter [7–10]. In contrast to free space, where bound dimers exist only in the BEC regime, two-dimensional (2D) confinement also stabilizes bound dimers in the BCS regime [1, 11]. The interplay between confinement-induced pairing and many-body physics in 2D confined mesoscopic systems of several hundred atoms has not been previously explored and offers new challenges for predictions [1, 3, 4].

We study a quasi-two dimensional Fermi gas of ⁶Li, where the ratio of the ideal gas transverse Fermi energy $E_{F\perp}$ to the energy level spacing $h\nu_z$ of the tightly confining potential is held nominally constant, with $E_{F\perp} \simeq 1.5 h\nu_z$. In this case, the system is not strictly 2D, but is far from 3D, as at most the first few oscillator states are relevant for many-body predictions [3]. Radio-frequency (rf) spectra are obtained for a 50-50 mixture of the two lowest hyperfine states denoted 1 and 2, by driving transitions to an initially empty hyperfine state 3 and measuring the depletion of state 2. At 720 G, well-below the Feshbach resonance, the 12 dimer binding energy E_b is larger than the local Fermi energy, and the observed spectra exhibit the expected threshold form, arising from dissociation of 12 dimers into 13 scattering (“free”) states. However, near the Feshbach resonance at 834 G, the measured spectra are not described by predictions for transitions between dimer states, nor by a two-parameter fit with fixed scaling of the initial and final state dimer energies. In this regime, where $E_{F\perp} > E_b$, polarons are expected

to be energetically more favorable than the corresponding dimers [12–14] and arise naturally for the initially empty final state [15]. Although we employ a balanced mixture, we find that the resonance locations can be described by transitions between noninteracting polaron states, i.e., an impurity atom in state 2 or in state 3, immersed in a bath of atoms in state 1, consistent with recent qualitative predictions for weakly attractive mixtures [15].

Prior experiments in the nearly 2D regime [6], $E_{F\perp} \ll h\nu_z$, yield rf spectra in agreement with predictions for a 2D gas [1]. In a simple BCS approximation to the rf spectrum in two dimensions at zero temperature, the trap-averaged rf transition rate to excite an atom from one populated state in a 50-50 mixture to an unpopulated noninteracting final state is $\propto \int_0^\infty d^2\mathbf{x}_\perp |\Delta|^2 \theta[\hbar\omega + \mu - \sqrt{\mu^2 + |\Delta|^2}]/\omega^2$. Here, ω is the radio frequency relative to the bare atomic transition frequency, μ is the chemical potential, and Δ is the pairing gap for the initial mixture. For a 2D gas, the BCS gap equation [1] gives $E_b = \sqrt{\mu^2 + |\Delta|^2} - \mu$, so that the predicted threshold for the spectrum is exactly the dimer binding energy [1, 6], in agreement with the measured spectral shifts after subtracting the known energy of the tightly bound final state pair [6]. In contrast, recent measurements of free-to-bound transitions in a quasi-2D Fermi gas of ⁴⁰K were interpreted in terms of dimers, but exhibited some discrepancies in the resonance locations [5], which have been interpreted in terms of 2D polarons [16, 17].

Table I lists the experimental parameters for several different magnetic fields and trap depths. The CO₂ laser standing-wave trapping potential is characterized by using parametric resonance in the weakly interacting regime near 300 G to determine the oscillation frequencies of the atoms in the transverse directions (ν_x, ν_y) and in the tightly confined axial direction (ν_z) . The axial trapping potential is taken to be $U_{axial} = U_0 \sin^2(2\pi z/\lambda)$, where the trap depth is readily determined from ν_z in the harmonic approximation, $U_0 = m(\nu_z \lambda)^2/2$. We find $\nu_\perp \equiv \sqrt{\nu_x \nu_y} = \nu_z/25$. The number of atoms per site is estimated using the lattice spacing of $5.3 \mu\text{m}$ and the number of atoms in the central

$B(G)$	$U_0(\mu K)$	$\nu_z(kHz)$	N_{site}	$E_{F\perp}(\mu K)$	E_b^{12}	E_b^{13}	ϵ_{bb}
719	27.5	26.0	1298	1.87	145	2.9	0.27
809	23.5	24.0	1951	2.12	12.6	0.88	0.53
810	294	85	1134	5.73	33.1	6.69	0.79
832	24.4	24.5	1620	1.97	7.25	0.81	0.66
832	274	82.0	1500	6.36	23.9	5.79	0.83
832	742	135	1800	11.47	39.1	12.45	0.89
831	1304	179	1250	12.65	51.9	18.9	0.91
842	24.4	24.5	1420	1.85	5.91	0.78	0.70
842	277	82.5	1617	6.64	21.4	5.66	0.85

TABLE I: Parameters for the radiofrequency spectra: Magnetic field B ; Trap depth U_0 ; Axial frequency ν_z ; Total number of atoms per pancake trap N_{site} ; Transverse Fermi energy $E_{F\perp} = \hbar\nu_\perp\sqrt{N_{site}}$; E_b^{12} and E_b^{13} are the dimer binding energies in kHz, for $\nu_\perp/\nu_z = 1/25$. The dimer binding energies are obtained using the Green's function method described in the supplementary material [18] for the scattering lengths $a(B)$ [19]; ϵ_{bb} is the corresponding bound dimer to bound dimer transition fraction [18].

part (along z) of the cloud, as measured by absorption imaging.

To compare the measured spectra to predictions, we begin by determining the 2D dimer binding energies, $E_b^{ij} \equiv \epsilon_b^{ij} \hbar\nu_z$ for atoms in states i and j , as described in the supplementary material [18] and given in Table I. The calculation includes the finite transverse confinement of the trapping potential, where $\nu_\perp/\nu_z = 1/25$, which significantly increases the dimer binding energy, especially for weakly bound dimers.

The contribution to the spectrum from a dimer-to-dimer transition is determined by computing the corresponding fraction ϵ_{bb} . In the weak binding approximation, including only the axial ground state part of the dimer wavefunction, we obtain,

$$\int d\nu I_{bb}(\nu) \equiv \epsilon_{bb}(q) = \frac{q^2}{4 \sinh^2(q/2)}, \quad (1)$$

where $q \equiv \ln(\epsilon_b^{13}/\epsilon_b^{12})$ for a $2 \rightarrow 3$ transition in a 12 mixture. In the supplementary material [18], we plot ϵ_{bb} as a function of magnetic field for both weak and tight binding.

Fig. 1 shows the measured spectra at 720 G, well below the Feshbach resonance, where the molecular dimer binding energy is larger than the local Fermi energy. At this field and trap depth, where the bound-to-bound transition fraction $\epsilon_{bb} = 0.27$, we expect bound-to-free transitions to dominate the resonance spectrum [18]. The resonance near 150 kHz is well fit by a threshold function for a quasi-two-dimensional gas using the calculated 12 and 13 dimer binding energies [18],

$$I_{bf}(\nu) = \frac{\epsilon_b^{12}\nu_z}{\nu^2} \frac{q^2 \theta(\nu - \epsilon_b^{12}\nu_z)}{\left[q - \ln\left(\frac{\nu}{\epsilon_b^{12}\nu_z} - 1\right) \right]^2 + \pi^2}, \quad (2)$$

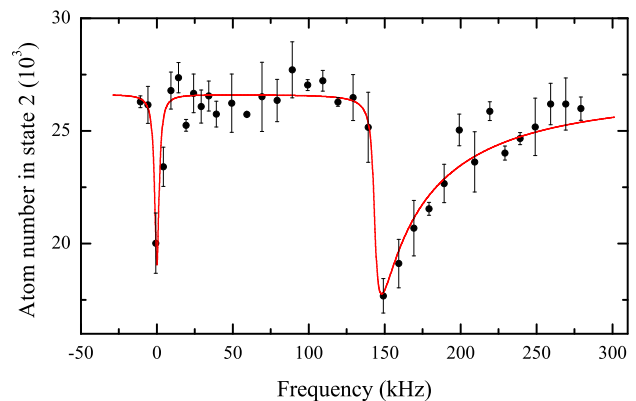


FIG. 1: RF spectra in a 1-2 mixture for a $2 \rightarrow 3$ transitions in a quasi-two-dimensional ${}^6\text{Li}$ Fermi gas near 720 G. The left resonance occurs at the bare atomic transition frequency and the threshold resonance spectrum on the right is in very good agreement with predictions for molecular dimers.

where ν is the rf frequency in Hz, relative to the bare atomic transition frequency, and $E_b^{12} = \epsilon_b^{12} \hbar\nu_z$ is the 12 dimer binding energy in Hz. Note that $\int d\nu I_{bf}(\nu) = 1 - \epsilon_{bb}(q)$, as it should.

Next, we examine spectra for the 12 mixture near the Feshbach resonance, at 832 G, Fig. 2, at 810 G, Fig. 3, and at 842 G, Fig. 4. For several of the spectra, the bare-atom resonance peak on the left side exhibits a fast rise and a tail toward higher frequency, which we assume arises from a density-dependent mean field shift [20]. At 832 G, the sharp threshold remains at nearly the same frequency (which we have set to 0 in Fig. 2), even when the trap depth is increased to maximum, where the ideal gas Fermi energy at the trap center is $E_{F\perp} = 12.7 \mu\text{K}$, i.e., $\simeq 260$ kHz. We assume that the threshold location is determined by the lowest density region at the cloud edges, where the mean field shift is negligible. The observed bare-atom resonance frequency is in agreement with that obtained at high temperature as well as for $2 \rightarrow 3$ transitions with all the atoms initially in the 2 state.

Near 834 G, for the conditions of our experiments, Table I shows that bound-to-bound transitions should dominate the spectrum above the bare atomic resonance frequency. To determine the frequency shift $\Delta\nu$, we fit lineshapes to each of the two resonances. A threshold lineshape is used for the bare-atom peak, which is convolved with a narrow Lorentzian. A Lorentzian with a larger width is used for second resonance. For the bare-atom resonance, the observed peak position is shifted to the right of the threshold location, which is determined from the fit. The results for $\Delta\nu$ are given in Table II and do not agree with the predictions for dimer-to-dimer transitions, $\hbar\Delta\nu_{dimer} = E_b^{12} - E_b^{13}$, shown as dashed lines in Figs. 2-4, and cannot be fit by $\hbar\Delta\nu_{dimer} = \lambda_{12} E_b^{12} - \lambda_{13} E_b^{13}$ for any fixed scale factors λ_{12} , λ_{13} .

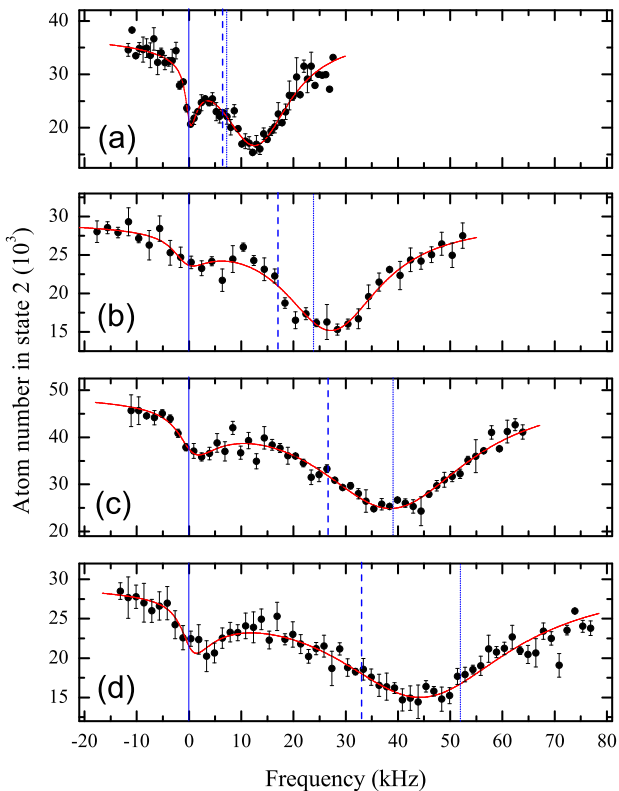


FIG. 2: RF spectra for a 1-2 mixture ($12 \rightarrow 13$ transition) near the Feshbach resonance at 834 G, versus trap depth U_0 . The atom number remaining in state 2 is shown versus rf frequency: a) $U_0 = 21 \mu\text{K}$, $\nu_z = 24.5$ kHz; b) $U_0 = 280 \mu\text{K}$, $\nu_z = 82.5$ kHz; c) $U_0 = 742 \mu\text{K}$, $\nu_z = 135$ kHz; d) $U_0 = 1304 \mu\text{K}$, $\nu_z = 179$ kHz. Vertical lines show the measured bare atomic resonance position (solid) and the predicted frequencies for confinement-induced dimers: bound-to-bound transition resonance $h\nu = E_b^{12} - E_b^{13}$ (dashed) and the threshold for the bound-to-free transition $h\nu = E_b^{12}$ (dotted). According to Table I, the bound-to-free transition (dotted line) should make a negligible contribution to the spectrum.

We consider the possibility that polarons and not dimers determine the primary spectral features, so that the difference between the initial and final state polaron energies determines the observed frequency shifts. We assume that the coherent part of the spectrum is approximately given by $Z \delta[\hbar\omega - E_p(3,1) + E_p(2,1)]$, where $E_p(i,1)$ is the polaron energy for an impurity atom in state $i = 2, 3$ immersed in a bath of state 1. Since the momentum does not change in the rf transition $Z \simeq Z_2 Z_3$ is determined by the overlap of the initial and final polaron momentum space wavefunctions [18]. For experiments at 832 G, we find that the individual polaron quasiparticle weights are $Z_2 > 0.8$ and $Z_3 > 0.9$ [18]. Therefore, we expect strong overlap between the initial and final polaron states, so that transitions between polaron states should make an important contribution to the spectrum.

We determine the 2D polaron energies for an isolated impurity atom in state 3 or state 2 in a bath of atoms

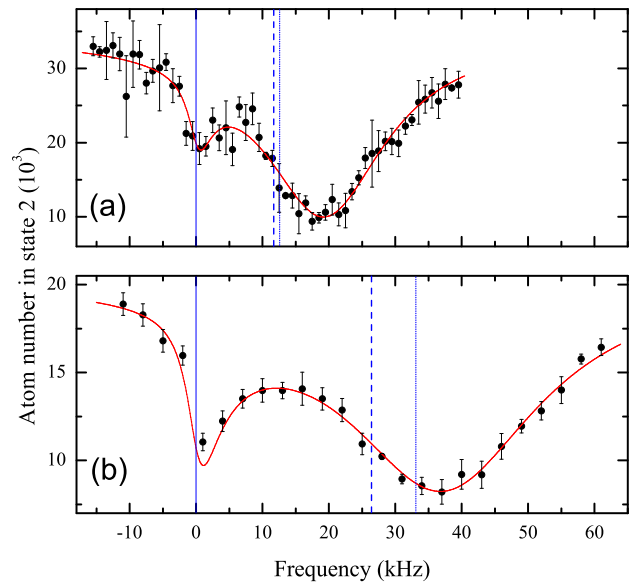


FIG. 3: RF spectra for $2 \rightarrow 3$ transitions in a quasi-two-dimensional ${}^6\text{Li}$ Fermi gas at 810 G: a) $U_0 = 23.5 \mu\text{K}$, $\nu_z = 24.0$ kHz; b) $U_0 = 294 \mu\text{K}$, $\nu_z = 85.0$ kHz. Vertical lines show the measured bare atomic resonance position (solid) and the predicted frequencies for confinement-induced dimers: bound-to-bound transition resonance $h\nu = E_{b12} - E_{b13}$ (dashed) and the threshold for the bound-to-free transition $h\nu = E_{b12}$ (dotted).

in state 1, using the method described in the supplementary material [18]. The method is based on that described for a 3D gas in the supplementary material of Schirotzek et al. [12], which utilizes the zero momentum polaron wavefunction proposed by Chevy [21]. We extend that method to the 2D problem, by renormalizing the interaction strength as in Refs. [1, 13, 14]. Using the calculated dimer binding energies to determine the polaron energies, we find that for an atom in state 3 at 832 G, the energy for an isolated polaron is attractive and more than half of the Fermi energy, much larger than the corresponding dimer binding energy. For an impurity in state 2, for which the 12 scattering length diverges, the polaron energy is attractive and somewhat larger than the Fermi energy. In this case, the polaron is localized to approximately the interparticle spacing, but is not small compared to the interparticle spacing, as it is at 720 G.

In calculating the polaron frequency shift, we assume the peak position is determined by the trap-averaged local Fermi energy E_F , which we take to be proportional to $E_{F\perp}$, the ideal gas global Fermi energy given in Table I, i.e., $E_F = \lambda_1 E_{F\perp}$, with λ_1 a fixed fit parameter. For $\lambda_1 = 0.67$, we obtain the polaron frequency shifts $h\Delta\nu_{\text{polaron}} \equiv E_p(3,1) - E_p(2,1)$, which are compared to the measurements in Table II. For the data just below and just above the resonance, at 810 and 842 G, Table II, we find excellent agreement. Further, at 832 G, the calculated polaron frequency shifts agree very well with the

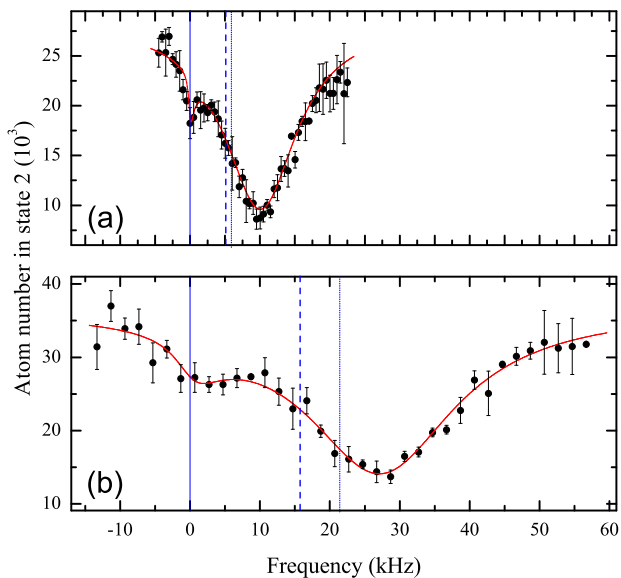


FIG. 4: RF spectra for $2 \rightarrow 3$ transitions in a quasi-two-dimensional ${}^6\text{Li}$ Fermi gas near 842 G: a) $U_0 = 24.4 \mu\text{K}$, $\nu_z = 25.0 \text{ kHz}$; b) $U_0 = 277 \mu\text{K}$, $\nu_z = 82.5 \text{ kHz}$. Vertical lines show the measured bare atomic resonance position (solid) and the predicted frequencies for confinement-induced dimers: bound-to-bound transition resonance $h\nu = E_{b12} - E_{b13}$ (dashed) and the threshold for the bound-to-free transition $h\nu = E_{b12}$ (dotted).

$B(\text{G})$	$\nu_z(\text{kHz})$	$\Delta\nu_{meas}(\text{kHz})$	$\Delta\nu_{polaron}(\text{kHz})$
809	24.0	18.7	18.3
810	85	37.1	37.0
842	24.5	10.1	9.7
842	82.5	27.2	26.7
832	24.5	12.3	11.6
832	82.0	28.3	29.1
832	135	38.8	42.8
831	179	44.5	48.3

TABLE II: Frequency shift $\Delta\nu$ between the bare atom peak and the second resonance peak for a 12 mixture near the Feshbach resonance. The corresponding axial trap frequency is ν_z . The measured values of $\Delta\nu$ are compared to the values calculated assuming a transition from a polaron in state 2 to a polaron in state 3, in a bath of atoms in state 1. The polaron frequency shifts are determined using the dimer binding energies, Table I, and the trap-averaged local Fermi energy $E_F = \lambda_1 E_{F\perp}$, where $E_{F\perp}$ is the ideal gas global Fermi energy, Table I, and $\lambda_1 = 0.67$ is a fit parameter.

measured frequency shifts at all four trap depths.

We have also obtained spectra for a 50-50 mixture of states 1 and 3 near the Feshbach resonance at 690 G, where we drive either the $13 \rightarrow 12$ transition or the $13 \rightarrow 23$ transition. In both cases, the binding energy of the final state 12 or 23 dimers is large compared to the local Fermi energy and suppresses the bound-to-bound

transition probability. For the Fermi energies used in the experiments, the observed threshold spectrum is not separated from the bare atom transition peak, so that dimer-to-free and polaron spectra could not be resolved. More theoretical work is needed to explain the detailed shapes and widths of all of the measured spectra, which may be improved in future experiments by local measurements [6].

In summary, we have observed rf spectra in a quasi-2D Fermi gas near a Feshbach resonance, where the transverse Fermi energy is comparable to the energy level spacing in the tightly confined direction. The spectra can be explained by transitions between noninteracting polaronic states, despite the 50-50 mixture employed in the experiments. These results support the conjecture [12] that a strongly interacting Fermi gas in a balanced mixture of two spin states is approximately a gas of noninteracting polarons.

This research is supported by the Physics Divisions of the Army Research Office, the Air Force Office of Sponsored Research, and the National Science Foundation, and the Division of Materials Science and Engineering, the Office of Basic Energy Sciences, Office of Science, U.S. Department of Energy. The authors thank Thomas Schäfer and Lubos Mitas for stimulating discussions.

-
- [1] M. Randeria, J.-M. Duan, and L.-Y. Shieh, Phys. Rev. Lett. **62**, 981 (1989).
 - [2] H. Moritz, T. Stöferle, K. Günter, M. Köhl, and T. Esslinger, Phys. Rev. Lett. **94**, 210401 (2005).
 - [3] J.-P. Martikainen and P. Törmä, Phys. Rev. Lett. **95**, 170407 (2005).
 - [4] G. Bertaina and S. Giorgini, Phys. Rev. Lett. **106**, 110403 (2011).
 - [5] B. Fröhlich, M. Feld, E. Vogt, M. Koschorreck, W. Zwerger, and M. Köhl, Phys. Rev. Lett. **106**, 105301 (2011).
 - [6] A. T. Sommer, L. W. Cheuk, M. J.-H. Ku, W. S. Bakr, and M. W. Zwierlein, Phys. Rev. Lett. **108**, 045302 (2012).
 - [7] K. M. O'Hara, S. L. Hemmer, M. E. Gehm, S. R. Granade, and J. E. Thomas, Science **298**, 2179 (2002).
 - [8] S. Giorgini, L. P. Pitaevskii, and S. Stringari, Rev. Mod. Phys. **80**, 1215 (2008).
 - [9] I. Bloch, J. Dalibard, and W. Zwerger, Rev. Mod. Phys. **80**, 885 (2008).
 - [10] W. Ketterle and M. W. Zwierlein, *Making, probing and understanding ultracold Fermi gases* (IOS Press, Amsterdam, 2008), in Ultracold Fermi Gases, Proceedings of the International School of Physics Enrico Fermi, Course CLXIV, Varenna, 20 - 30 June 2006.
 - [11] D. S. Petrov and G. V. Shlyapnikov, Phys. Rev. A **64**, 012706 (2001).
 - [12] A. Schirotzek, C.-H. Wu, A. Sommer, and M. W. Zwierlein, Phys. Rev. Lett. **102**, 230402 (2009).
 - [13] S. Zöllner, G. M. Bruun, and C. J. Pethick, Phys. Rev. A **83**, 021603(R) (2011).
 - [14] M. M. Parish, Phys. Rev. A **83**, 051603 (R) (2011).

- [15] V. Pietilä (2012), arXiv:1203.6054v1[cond-mat.quant-gas].
- [16] R. Schmidt, T. Enss, V. Pietilä, and E. Demler, PRA **85**, 021602(R) (2012).
- [17] We thank M. Köhl for providing a preprint of his group's new experimental work on 2D polarons arXiv:1203.1009v1 [cond-mat.quant-gas], following submission of our paper arXiv:1201.3560v1 [cond-mat.quant-gas].
- [18] See the supplementary material.
- [19] M. Bartenstein, A. Altmeyer, S. Riedl, R. Geursen, S. Jochim, C. Chin, J. H. Denschlag, R. Grimm, A. Simoni, E. Tiesinga, et al., Phys. Rev. Lett. **94**, 103201 (2005).
- [20] C. Langmack, M. Barth, W. Zwerger, and E. Braaten (2011), arXiv:1111.0999v1 [cond-mat.quant-gas].
- [21] F. Chevy, Phys. Rev. A **74**, 063628 (2006).